HHS Public Access

Author manuscript

Curr Biol. Author manuscript; available in PMC 2019 March 15.

Published in final edited form as:

Curr Biol. 2017 October 09; 27(19): 2940–2950.e4. doi:10.1016/j.cub.2017.08.042.

Spatial auxin signaling controls leaf flattening in *Arabidopsis*

Chunmei Guan[1], **Binbin Wu**[1,2], **Ting Yu**[1,3], **Qingqing Wang**[1,2], **Naden T. Krogan**[4], **Xigang Liu**[5], and **Yuling Jiao**[1,2,*]

[1]State Key Laboratory of Plant Genomics, Institute of Genetics and Developmental Biology, Chinese Academy of Sciences, and National Center for Plant Gene Research, Beijing, 100101, China

[2]College of Life Sciences, University of Chinese Academy of Sciences, Beijing, 100049, China

[3]College of Agronomy, Northwest A&F University, Yangling, Shaanxi, 712100, China

[4]Department of Biology, American University, Washington, DC, 20016, USA

[5]State Key Laboratory of Plant Cell and Chromosome Engineering, Center for Agricultural Resources Research, Institute of Genetics and Developmental Biology, Chinese Academy of Sciences, Shijiazhuang, 050021, China

SUMMARY

The flattening of leaves to form broad blades is an important adaption that maximizes photosynthesis. However, the underlying molecular mechanism of this process remains unclear. The *WUSCHEL-RELATED HOMEOBOX* (*WOX*) genes *WOX1* and *PRS* are expressed in the leaf marginal domain to enable leaf flattening, but the nature of *WOX* expression establishment remains elusive. Here we report that adaxial-expressed MONOPTEROS (MP) and abaxial-enriched auxin, together, act as positional cues for patterning the *WOX* domain. MP directly binds to the *WOX1* and *PRS* promoters and activates their expression. Furthermore, redundant abaxial-enriched ARF repressors suppress *WOX1* and *PRS* expression, also through direct binding. In particular, we show *ARF2* is redundantly required with *ARF3* and *4* to maintain the abaxial identity. Taken together, these findings explain how adaxial-abaxial polarity patterns the mediolateral axis and subsequent lateral expansion of leaves.

Graphical Abstract

*Lead Contact and Correspondence: yljiao@genetics.ac.cn.

AUTHOR CONTRIBUTIONS

Y.J. and C.G. designed the research. C.G., B.W., T.Y. and Q.W. performed the research. C.G., B.W. and Y.J. analyzed the data. N.T.K. and X.L. provided reagents. Y.J. and C.G. wrote the paper with input from N.T.K.

SUPPLEMENTAL INFORMATION

Supplemental Information includes six figures and one table and can be found with this article online.

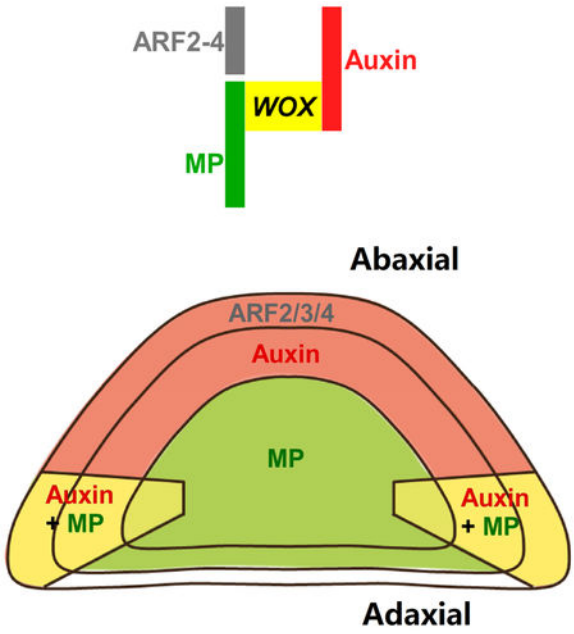

eTOC Blurb

The flattening of leaves to form broad blades is an important adaption. Guan et al. show that the adaxial-expressed *MP,* abaxial-enriched auxin, and abaxial-expressed *ARF* repressors together position *WOX* expression in the middle domain. This finding describes how adaxial-abaxial polarity patterns the mediolateral axis and thus leaf flattening.

Keywords

leaf; auxin; ARF; WOX; patterning

INTRODUCTION

The flattening of leaves to form broad blades is an important adaption that maximizes photosynthesis. Following initiation from the shoot apical meristem (SAM), leaf primordia develop three axes of asymmetry, a proximodistal axis, an adaxial-abaxial axis, and a mediolateral axis, to form planar leaves. Patterning the mediolateral axis (from the midrib to the margin) promotes leaf blade outgrowth, and depends on adaxial-abaxial patterning (also known as dorsoventral, or up-down polarity) [1].

Extensive molecular genetic studies have identified a transcriptional regulatory network containing leaf abaxial- and adaxial-promoting genes [2-7]. Adaxial-abaxial polarity establishment requires domain-specific expression of these transcription factors and small RNA encoding genes. It has been proposed that incipient leaf primordia may be prepatterned into adaxial and abaxial domains [6]. Regulatory genes expressed in the abaxial domain suppress those expressed in the adaxial domain and *vice versa.* In particular, the adaxial-expressed mobile trans-acting small interfering RNA3 (*TAS3*) forms a gradient [8], and restricts its targets, *AUXIN RESPONSE FACTOR3* (*ARF3*, also known as *ETTIN*) and

ARF4, to the abaxial domain [9-11]. Likewise, abaxial-expressed *MicroRNAs 165* and *166* (*miR165/166*) form an opposite gradient [12-14], and restrict the expression of class III homeodomain leucine zipper (HD-ZIP III) genes *PHABULOSA, PHAVOLUTA,* and *REVOLUTA* to the adaxial domain [15, 16]. These and additional mutual repression and positive regulatory interactions confine and stabilize gene expression regions to fine-tune adaxial-abaxial polarity. In addition to gene expression, auxin transport leads to a transient adaxial low auxin domain that is required for adaxial-abaxial patterning [17].

The adaxial-abaxial polarity establishment promotes leaf blade outgrowth, and this mediolateral axis growth requires the activity of leaf meristems (also called marginal blastozones) [18-20]. Although leaves are determinate organs and do not contain anatomical features typical of meristems, transient leaf meristems, which are restricted to the marginal domains, enable leaf blade expansion [21]. Expression of *WUSCHEL-RELATED HOMEOBOX1* (*WOX1*) and *PRESSED FLOWER* (*PRS*)/*WOX3* of *Arabidopsis* in the marginal domain (also called the middle domain) between the adaxial and abaxial domains is critical for leaf blade outgrowth [22, 23]. *WOX1* homologs in maize, petunia, *Medicago,* and tobacco have similar expression patterns and control leaf blade outgrowth [23-25]. *WUSCHEL* (*WUS*), which is required for the SAM [26], can substitute for *WOX1* and *PRS* functions in the leaf [27, 28], and *vice versa* [29], suggesting similarities between leaf meristems and the SAM.

WOX expression in the leaf marginal domain enables leaf flattening, but little is known about how the expression domain of *WOX* genes is established. In fact, we also know little about the nature of activation of other stem cell-promoting *WOX* genes. In this study, we found that the recently identified abaxial auxin maxima work with domain-specific ARF activators and repressors to precisely activate *WOX1* and *PRS* expression in the marginal domain, thus defining the *WOX* domain for leaf blade outgrowth.

RESULTS

Spatially refined auxin signaling in the middle domain of young leaf primordium

We have recently shown that transient abaxial-enriched auxin distribution contributes to leaf patterning [17]. We sought to identify downstream targets of auxin signaling that regulate leaf patterning. ARF transcription factors are important auxin signaling mediators. Therefore, we first analyzed ARF expression patterns during early leaf development to understand spatial auxin signaling.

MONOPTEROS (MP) is an ARF that regulates the expression of auxin responsive genes, and has been recently shown to regulate leaf development [17, 30]. A functional *pMP::MP-GFP* fluorescent marker shows that *MP* is expressed in young leaf primordia, and becomes obviously adaxially expressed after P_2, which designates the second youngest primordium (Figure 1A, S1A, and S1C). In P_3 and P_4, *MP* expression is found in the middle domain, covering the marginal domains, and part of the adaxial domain. In addition, the expression domain of *MP* expands from the apex to base from P_2 to P_4, consistent with the basiplastic gradient of leaf expansion in *Arabidopsis* [31]. In addition to MP, there are four other ARF activators, NONPHOTOTROPIC HYPOCOTYL4 (NPH4)/ARF7, ARF6, 8 and 19, in

Arabidopsis [32]. All these ARFs have expression in the adaxial domain to different extents in young leaf primordia (Figure S1B).

ARFs activate auxin signal transduction in response to auxin. Consistent with a previous report [17], the auxin signaling sensor DII-Venus, whose signal indicates low auxin, is enriched in the adaxial side of the tip region, indicating reduced auxin levels in this domain from P_2 to P_4 (Figure 1B and S1C). Nevertheless, dispersed DII-Venus signal was also detected at a low frequency in the epidermis. By contrast, the non-responsive mDII-Venus control has uniform expression in early leaf primordia [33]. To precisely compare auxin distribution and signaling, we crossed the auxin signaling reporter *pDR5::GFP-ER* with *p35S::DII-Venus.* In plants co-expressing the two markers, we detected GFP signals in the marginal domain, initially in the tip and then expanded toward the base (Figure 1B). On the other hand, an alternative auxin signaling reporter, DR5v2 [34], had more broad expression in leaf primordia (Figure S1D). The *MP* expression domain partially overlaps with both DR5 and DII-Venus domains. Thus the spatial distributions of auxin and MP, as well as additional ARF activators, lead to refined auxin signaling in the marginal domain. We detected the expression of *WOX1* and *PRS* in the marginal domain [22, 23] (Figure 1C and 1D), completely covered the DR5 regions. Thus, *WOX1* and *PRS* expression overlaps with auxin signaling maxima in the leaf marginal domain.

MP acts in leaf blade outgrowth and regulates *WOX1* and *PRS* expression

Previous studies have shown that ectopic MP activity leads to defective leaf development [17, 30]. To test if MP is involved in normal leaf development, we analyzed the leaf phenotype in *arf5-1*, a strong *MP* mutant allele. The cotyledons and rosette leaves of five-day-old *arf5-1* mutant were narrower than wild-type leaves (Figure 2A and 2B). Furthermore, after growing for 17 days, about 7.5% (3/40) of *arf5-1* mutants form needle-like rosette leaves that fail to flatten (Figure 2C and 2D). The frequency of needle-like lateral organs was substantially increased to ~100% in the *mp-G12 nph4-1* mutant (Figure 2E and 2F), suggesting redundant roles of *NPH4* with *MP* in leaf development. These results indicated that *MP* is involved in normal leaf development, especially leaf flattening.

Because *WOX1* and *PRS* expression overlaps with auxin signaling in the marginal domain, and MP-mediated auxin signaling regulates leaf flattening, we speculated that MP and related ARF activators promote *WOX* expression. To this end, we first analyzed *PRS* expression in the *mp nph4* mutant leaves. The detection of *FILAMENTOUS FLOWER* (*FIL*) confirmed that the needle-like structure had lateral organ identity [35] (Figure 2G). However, we could not detect *PRS* expression in the needle-like lateral organs (Figure 2H).

Because leaf development is severely compromised, we also made a presumably dominant-negative *MP* to understand its role in regulating *WOX* expression and leaf flattening. We expressed a constitutively repressive fusion protein of MP, which lacks domains III and IV and is fused to an ETHYLENE RESPONSE FACTOR-associated Amphiphilic Repression (EAR) motif and a GR domain (termed MPΔ-EAR-GR), under the endogenous *MP* promoter. The deletion of domains III and IV makes the fusion protein escape auxin regulation [30], and the EAR domain converts MP into a transcriptional repressor [36], so that the MPΔ-EAR-GR fusion protein constitutively represses target gene expression, and

thus auxin signaling, after dexamethasone (Dex) induction. Using *Dof5.8,* a previously reported direct target gene of MP [37], we confirmed that the MPΔ-EAR-GR fusion protein could suppress target gene expression as designed (Figure S2A). We found that Dex induction resulted in narrower leaves suggesting a reduction of the leaf blade outgrowth (Figure 2I and S2B), reminiscent of the phenotypes observed in *wox1 prs* mutants [22, 23]. Furthermore, we found that a 4 hr Dex induction of MPΔ-EAR-GR resulted in a downregulation of *WOX1* and *PRS* expression (Figure 2J). Taken together, these results indicated that MP promotes *WOX1* and *PRS* expression and leaf flattening.

Ectopic adaxial *WOX1* and *PRS* expression leads to defective leaf flattening

Previous studies have shown that *MPΔ,* which escapes auxin regulation and becomes constitutively active without auxin, leads to severe defects in leaf adaxial-abaxial polarity development [17, 30]. We went on to test if this polarity defect is caused by ectopic *WOX1* and *PRS* expression. In transgenic *pMP::MPΔ* plants, leaf blade outgrowth (i.e. mediolateral axis expansion) is reduced but blade thickness is increased, suggesting ectopic adaxial-abaxial expansion (Figure 3A and H). In addition, small blade outgrowths appear on the adaxial leaf surface, a phenotype also observed in *WOX1* overexpressing leaves [22]. An RT-qPCR assay indicated that *WOX1* and *PRS* expression in *pMP::MPΔ* plants increased 3- and 10-fold higher, respectively, compared to the wild-type (Figure 3B). To further test if forced adaxial auxin signaling is sufficient to trigger *WOX1* and *PRS* expression, we expressed *MPΔ* in the adaxial epidermis from the *AS2* promoter. We observed comparable upregulation of *WOX1* and *PRS* expression in*pAS2::MPΔ* plants (Figure 3B). An *in situ* hybridization (ISH) analysis revealed that the *WOX1* and *PRS* expression domain expanded from the middle domain into the adaxial domain in *pMP::MPΔ* leaf primordia (Figure 3C and S3B). We also tested if auxin treatment can upregulate *WOX* expression in leaves. The structure of the *Arabidopsis* shoot apex prohibited access to early primordia, where auxin treatment is functional. To this end, we used tomato shoot apices with larger leaf primordia. We found the homologous *SlWOX1* expression was upregulated after a 24 h IAA treatment (Figure S3A). These results indicated ectopic adaxial *MP* activation induced ectopic adaxial *WOX* gene expression, further supporting that MP activates *WOX1* and *PRS* expression.

To test if ectopic *WOX* expression causes leaf polarity development defects, we crossed the *pMP::MPΔ* transgenic plants with *wox1-2* or*prs* mutants. Whereas both *wox1-2* and *prs* single mutant leaves show no obvious phenotypes, *wox1-2 prs* double mutant leaves are narrower than wild-type leaves [22, 23]. Introduction of either *wox1-2* or *prs* could partially, but significantly, restore leaf expansion in *pMP::MPΔ* (Figure 3D and 3F-3H), although the expression level of *MPΔ* was comparable in the *wox1-2* background and even higher in the *prs* background (Figure 3E). We could not obtain *pMP::MPΔ wox1-2prs* plants. Because we observed a high frequency of seed abortion in *pMP::MPΔ wox1-2 prs*/+ siliques, ectopic *MPΔ* may lead to defective embryogenesis in the *wox1-2 prs* background. The results indicated that the ectopic adaxial *MP* activity, which is otherwise suppressed due to lack of auxin, induces ectopic *WOX1* and *PRS* expression to alter normal leaf patterning.

MP directly upregulates *WOX1* and *PRS* expression

To investigate whether the MP protein directly induces *WOX1* and *PRS* expression, we constructed a Dex-inducible *pMP::MPΔ-GR* line. Activation of MPΔ-GR by Dex application led to an inhibition of blade outgrowth and ectopic adaxial-abaxial axis thickening (Figure 4A), which is similar to *pMP::MPΔ* leaves (Figure 2I). An RT-qPCR analysis indicated that Dex induction of MPΔ-GR triggered *WOX1* and *PRS* expression up-regulation within 4 hr (Figure 4B). We could also detect *WOX1* and *PRS* induction with the presence of cycloheximide (CHX), an inhibitor of protein biosynthesis, suggesting that induction of *WOX1* and *PRS* does not require *de novo* protein synthesis and that these genes are likely direct targets of MP.

An analysis of the *WOX1* and *PRS* promoter regions identified multiple auxin-response element (AuxRE) core motifs, which are sufficient for ARF recruitment [32] (Figure 4C). In particular, we found one AuxRE pair in the *WOX1* promoter region, and two pairs in the *PRS* promoter region. Although AuxRE pairs may not be necessary for MP binding, such pairs have been identified in a few known MP target genes [38], making them good candidates as MP binding sites.

To determine whether MP associates with the promoters of *WOX1* and *PRS in vivo,* we performed chromatin immunoprecipitation (ChIP) assays using *pMP::MP-GFP* and *pMP::MP-HA* transgenic lines [39]. Using a series of primer pairs distributed over the *WOX1* and *PRS* promoters covering AuxRE motifs (Figure 4C), we found that MP binds 1200 base pairs (bp) upstream of the *WOX1* start codon and 1500 bp upstream of the *PRS* start codon positions which both contain AuxRE pairs (Figure 4D and 4E).

A yeast one hybrid (Y1H) assay further confirmed that MP bound to the upstream promoter fragments containing AuxRE pairs identified by ChIP assay, but not other AuxRE motif-containing ones (Figure 4F). The additional weak binding regions detected by ChIP assays may imply that MP associates with other regions by interacting with transcription factors that binds to other elements. We performed transient expression assays using *Nicotiana benthamiana* leaves to further test effects of MP on *pWOX1::firefly luciferase* (*Luc*) reporter expression. We observed that MP promotes expression of *pWOX1::Luc* (Figure 4G-4I). Taken together, our results indicated that MP activates *WOX1* and *PRS* expression through direct binding to their promoter regions.

To test if the AuxRE bound by ARFs in the *WOX1* promoter region is critical for *WOX1* activity, we made specific deletions of this region. When we fused *WOX1* to its intact endogenous promoter, and transformed into *wox1-2 prs* mutant plants, the vast majority of the obtained transgenic lines (95%, 55/58) were rescued to wild-type-like leaf shape (Figure 4J, 4K and S4). However, deletion of the AuxREs led to a substantial portion of the transgenic lines (33%, 20/61) unable to rescue the leaf flattening defect of *wox1-2 prs* plants (Figure 4J, 4K and S4). This result further confirms the important role of the AuxRE region in regulating *WOX1* activity.

ARF2, *ARF3* and *ARF4* suppress *WOX1* and *PRS* expression in the abaxial domain

Previous studies have shown that *ARF3* and *ARF4* promote leaf abaxial identity [9-11]. Both *ARF3* and *ARF4* are targets of ta-siRNAs derived from the adaxial expressed *TAS3* gene [10], and their expression is restricted to the abaxial domain [11]. A careful analysis indicated that ARF3 has relatively uniform expression in P_1 and P_2 stages and is restricted to the abaxial domain in the P_3 stage (Figure 1E). *TAS3* derived ta-siRNAs also targets *ARF2* [40, 41], although the *arf2* mutation alone causes no organ asymmetry phenotype [42, 43]. *ARF2, ARF3,* and *ARF4* all encode transcriptional repressors [32], and they bind to the same AuxRE sequence as ARF activators [38, 44], leading to the hypothesis that these three ARF repressors redundantly regulate *WOX* expression, antagonistic to MP.

To test whether these ta-siRNA-targeted *ARF* genes regulate *WOX1* and *PRS* expression, we first checked *WOX* gene expression in *arf2-6,* and *arf3-1 arf4-2* mutants, as well as in *ARF2* overexpression transgenic plants (*ARF2ox*), respectively (Figure 5A-D). The expression of *WOX1* and *PRS* increased in both *arf* mutant backgrounds, and mildly decreased in the *ARF2ox* transgenic plants. Further ISH analyses revealed that the *WOX1* and *PRS* transcript accumulation expanded into the abaxial domain in *arf3-1 arf4-2* leaf primordia (Figure 5B and S5A). These results indicated that these *ARFs* negatively regulate the expression of *WOX* genes.

To determine whether *ARF2* is involved in leaf development, we compared the cross sections of *arf2-6* and *ARF2ox* rosette leaf blades with that of wild-type plants (Figure 5E). In wild-type leaves, there is a steep contrast of adaxial and abaxial mesophyll morphology: Cells in the adaxial two layers are larger, round, and densely packed, whereas cells in the abaxial two layers are more branched and are separated by spacious air spaces. In *arf2-6,* abaxial mesophyll cells are less branched, and all mesophyll cells in *ARF2ox* are round-shaped. Furthermore, we constructed *arf2-6 arf3-1 arf4-2* triple mutant plants (Figure 5F, S5B and S5C). Whereas *arf3-1 arf4-2* leaves have mild leaf polarity defects [11], *arf2-6 arf3-1 arf4-2* leaves have more severe leaf patterning defects when plants are mature (~20 d after germination). We observed frequent deep lobes and occasional trumpet-like leaves in the triple mutant but not the double mutant. In addition, there are more adventitious small blade protrusions on the abaxial side in the triple mutant. We also designed an artificial miRNA (amiRNA) targeting *ARF2, ARF3* and *ARF4* [45], *amiR-ARF,* and constitutively expressed it under the control of the Cauliflower Mosaic Virus *35S* promoter (*p35S*). Leaves of *p35S::amiR-ARF* lines resemble the observed *arf3-1 arf4-2* leaf phenotypes (Figure S6A and S6B), possibly due to residual expression of any of the three ta-siRNA-targeted ARFs (Figure S6C). In summary, *ARF2* is redundantly involved in leaf polarity development along with *ARF3* and *ARF4*.

To reveal whether the three ta-siRNA-targeted ARFs directly suppress *WOX1* and *PRS* expression, we used a Dex inducible *pARF3::mARF3-GR* line, which has *TAS3*-independent *ARF3-GR* expression [46]. We measured the effect of ARF3 activation in *pARF3::mARF3-GR* plants on *WOX1* and *PRS* expression by RT-qPCR. ARF3 activation resulted in rapid reduction of both *WOX1* and *PRS* transcripts levels within 4 hr, in the absence or presence of the protein synthesis inhibitor CHX (Figure 6A), suggesting direct transcriptional suppression. We further performed ChIP and Y1H assays to confirm direct

binding of ARF3 to *WOX1* and *PRS* promoter regions and to test if ARF2 and ARF4 also bind to the same regions. ChIP results indicated that ARF3 bound to the *WOX1* and *PRS* promoters (Figure 6B). The Y1H experiments suggested that all three ARFs bound to the MP-bound promoter regions of *WOX1* and *PRS* (Figure 6C and 6D). Both regions harbor one or two AuxRE pairs. Taken together, these results support that the three ARF repressors redundantly suppress *WOX1* and *PRS* expression by directly binding to their promoter regions that are also targeted by MP.

MP and ARF3 play antagonistic roles in regulating *WOX1* promoter activity

Since MP and ta-siRNA-targeted ARF repressors have opposite effects on *WOX1* and *PRS* expression (Figures 2-5), and all these ARFs can bind to the same promoter regions (Figures 4 and 6), we speculated that ARF activators and ARF repressors compete for access to *WOX1* and *PRS* promoters and thereby refine spatial expression of *WOX1* and *PRS* in the leaf marginal domain. To test this hypothesis, we performed transient expression assays using *Nicotiana benthamiana* leaves to test effects of MP and ARF3 on *pWOX1::Luc* reporter expression. We observed that MP promotes *pWOX1::Luc* reporter expression, and ARF3 interfered with MP activation of *pWOX1::Luc* expression (Figure 7A-C). Thus, ARF3 as a repressor antagonizes MP activation of *WOX1* expression, presumably through competing for access to the same promoter regions.

ARF2, *ARF3* and *ARF4* contribute to leaf blade outgrowth

To further understand the genetic interactions between the ta-siRNA-targeted *ARF* genes and *WOX* genes, we introduced *p35S::amiR-ARF* into *wox1-2 prs.* Suppression of *ARF2, ARF3* and *ARF4* expression further enhanced the leaf blade outgrowth defect of *wox1-2 prs* (Figure 5G-5I). We observed a ‘bladeless’ phenotype at high frequency (Figure 5G and 5H), that resembles the classical *lam1* mutant of *Nicotiana sylvestris* [47]. Thus, these ta-siRNA-targeted *ARF* genes also contribute to leaf blade outgrowth, especially when *WOX* activity is missing. The *wox1-2 prs p35S::amiR-ARF* leaves are radially symmetric (Figure 5I), which is also observed in *lam1* and related *Medicago stf* mutant [24, 47]. In contrast to tobacco, *Medicago* and maize, *Arabidopsis wox1 prs* mutants only have mild leaf blade outgrowth phenotype. These ta-siRNA-targeted *ARF* genes may provide the remaining leaf blade outgrowth activity.

DISCUSSION

Leaf flattening promotes efficient photosynthesis, and is an excellent model to study organ patterning. Although leaves exhibit determinate growth with a finite period of development, it has long been proposed that leaves also require meristem activity that ensures cell proliferation [18-21]. Similar to the SAM and the root apical meristem (RAM), leaf meristems have active proliferative activity to produce cells that further differentiate to enable leaf blade outgrowth. Notably, leaf meristems share highly conserved genes with the SAM and RAM. The *WOX* genes, which are key for maintaining stem cells both in SAM and RAM, are also expressed in the leaf meristems [22-25]. *WOX1* and *PRS* for the leaf meristems and *WUS* for the SAM are partially interchangeable [27-29], further supporting the similarity between leaf meristems and the SAM. Unlike the apical meristems, leaf

meristems do not maintain indeterminate self-renewal and cell proliferation. Cell division ceases in leaves after a certain time period, similar to the floral meristem. Thus, leaf patterning, especially flattening, depends on activities of leaf meristems.

It has long been proposed that the establishment of adaxial-abaxial polarity conditions establishment of the mediolateral axis and subsequent leaf flattening [1]. By showing how *WOX* expression is defined, our study establishes a molecular link between the two axes (Figure 7D). Auxin is depleted from the adaxial domain during early leaf development [17]. On the other hand, MP (and possibly other ARF activators) is expressed in the adaxial and marginal domains right after leaf initiation (P_2 in Figure 1A and S1C). The combination of auxin and ARF activator distribution results in restricted auxin signaling in the marginal domain (Figure 1B). In the root, HD-ZIP III transcription factors activate *MP* expression [48]. The same HD-ZIP IIIs are expressed in the leaf adaxial domain, and may set up the initial adaxial-enriched *MP* expression. Because auxin signaling promotes *MP* expression [49], this positive feedback loop may further refine *MP* expression to the marginal domain (Figure 1A). MP promotes the expression and polarization of the auxin efflux carrier PIN-FORMED1 [49, 50], further reinforcing the positive feedback loop and the marginal auxin signaling maxima. Nevertheless, weak auxin signaling may also exist in other regions, as suggested by the uniform DR5v2 expression (Figure S2D). DR5v2 is expected to be more sensitive to low level auxin signaling than the classical DR5 reporter [34].

Our genetic and molecular analysis indicated that the marginal auxin signaling activates *WOX1* and *PRS* expression (Figures 3 and 4), mediated by direct binding of MP to *WOX* promoter regions (Figure 4). Furthermore, the three abaxially expressed ta-siRNA-targeted ARFs, which are transcriptional repressors [32], suppress *WOX1* and *PRS* expression in the abaxial domain by binding to the same AuxRE-containing promoter elements targeted by MP (Figures 4-6). Recent structural analysis showed that both MP and ARF1, another ARF repressor, each form homodimers and bind to related AuxRE pairs [38]. It is conceivable that ARF repressors compete with ARF activators to restrict *WOX* expression. Albeit both under auxin signaling regulation, the expression domains of *PRS* and *WOX1* do not fully overlap (Figure 1C and 1D) [22], suggesting additional regulators further specify their expression.

Our results also indicated that the three abaxially expressed ta-siRNA-targeted ARF repressors may regulate leaf patterning at two levels. The three ARF repressors promote the abaxial fate and restrict *WOX* expression (Figure 5B). Loss of these ARF repressors lead to adventitious small blade protursions on the abaxial side, which is associated with ectopic abaxial *WOX* activities (Figure 5F, S5 and S6) [11]. In addition, the abaxial-expressing ARF repressors may also contribute to leaf blade outgrowth. Introducing *amiR-ARF* into the *wox1 prs* double mutant lead to synergistic effect (Figure 5G-5I). The *wox1 prs amiR-ARF* plants showed a ‘bladeless’ phenotype, suggesting strongly enhanced mediolateral growth defects. Thus, these *ARF* repressor genes also contribute to leaf blade outgrowth. In contrast, loss of *WOX* activity alone is sufficient to induce a ‘bladeless’ phenotype in tobacco and *Medicago* [24, 47], suggesting different contributions of *ARF* repressors to leaf blade outgrowth in different plant species.

Overall, our analyses show that the adaxial-abaxial distribution of auxin, ARF activators, and ARF repressors collectively defines *WOX1* and *PRS* expression, and the leaf meristem to the marginal domain. The leaf marginal meristem enables leaf expansion, and establishes the mediolateral axis [22, 24]. Finally, the leaf marginal meristem is gradually suppressed by multiple NGATHA (NGA) and CINCINNATA-class-TCP (CIN-TCP) transcription factors, resulting in determinate leaf growth [21].

STAR★Methods

Contact for Reagent and Resource Sharing

Further information and requests for resources and reagents should be directed to and will be fulfilled by the Lead Contact, Yuling Jiao (yljiao@genetics.ac.cn).

Experimental Model and Subject Details

Growth conditions—*Arabidopsis thaliana* plants were grown in soil under constant light at 22°C. For imaging and ISH, seeds were stratificated for 2 d on 1/2 Murashige and Skoog (MS) medium (Duchefa), 1% (w/v) sucrose, and 0.8% (w/v) agar in the dark at 4°C and then under short-day conditions (8 hr light/16 hr dark) for 15 d.

Genetic material—The *Arabidopsis thaliana* ecotypes Columbia (Col-0) and Landsberg *erecta* (L*er*) were used as the wild-types. The *arf5-1, mp-G12 nph4-1* [50], *arf2-6* (CS24600) [42], *arf3-1* (CS24603) [43], *arf4-2* (SALK_070506C) [11], *wox1-2* (8AAJ85), and *prs* (SALK_127850) [23] mutants used in this study are in the Col-0 background. The transgenic lines *pARF6::n3GFP, pARF8::n3GFP, pARF19::n3GFP,* and *pNPH4::n3GFP* [51], *p35S::DII-Venus* [52], *pDR5::GFP-ER* [53], *pDR5v2::ntdTomato pDR5::n3GFP* [34], *pMP::MP-GFP, pMP::MP-HA* [39], *pMP::MPΔ* [17], *pWOX1::SV40-3XGFP, pPRS::SV40-3XGFP* [54], and *ARF2ox* [55] are in Col-0, and *pARF3::ARF3-GFP* and *pARF3::mARF3-GR* are in L*er* [46].

Method Details

Construction of transgenic plants—To construct *pMP::MPΔ-GR*, a 6,695-bp *MP* genomic DNA fragment (containing 3,231 bp upstream and 3,461 bp downstream of the start condon, respectively) was amplified using the forward primer MP-F and the reverse primer MP-R and fused in-frame to GR through cloning between the *Xho*I and *Xba*I sites of the binary vector pG0229. To construct *pMP::MPΔ-EAR-GR*, a 120-bp fragment coding for 183-222 amino acids of *AtERF4* was amplified using the primer AtERF4-F and AtERF4-R and fused to the C-terminus of *pMP::MPΔ* through the *Sac*I site in the pEASY-Blunt vector (TransGen). The resulting fusion gene was cloned between the *Xho*I and *Xba*I sites of the binary vector pG0229. These constructs were transformed into Col-0 plants, and more than 10 independent stable transgenic lines were characterized for each construct.

To construct *pWOX1::WOX1-mCherry*, a 6,482-bp *WOX1* genomic fragment (containing 4,456 bp upstream and 2,023 bp downstream of the start condon, respectively) was amplified using the forward primer WOX1-F and the reverse primer WOX1-R and fused in-frame to mCherry through cloning between the *BamH*I and *Xho*I sites of the binary vector

pYBA1128. To obtain the *pWOX1Δ::WOX1-mCherry* construct, a 142-bp fragment (1,347-bp to 1,205-bp upstream of the start codon) was deleted using PCR and the deleted version of *WOX1* genomic fragment was cloned into pYBA1128 between the *BamH*I and *Xho*I sites. The two constructs were transformed into *wox1-2 prs* double mutants, and more than 50 independent stable transgenic lines were characterized for each construct.

For transformation of *Arabidopsis* plants, *Agrobacterium tumefaciens* strain GV3101 and floral dip method were used in all the transformation experiments [56].

RNA extraction and RT-PCR—Total RNA was extracted from inflorescences or leaves using the RNeasy Micro kit (Qiagen) according to the manufacturer's instructions. For Dex/CHX treatment experiments, transgenic shoot apexes were treated by 10 μM Dex alone or with 10 μM CHX for 4 hr. The first strand of cDNA was synthesized using TransScript One-Step gDNA Removal and cDNA synthesis SuperMix (TransGen), and then used as templates for reverse transcription quantitative PCR (RT-qPCR). RT-qPCR was performed through the Bio-Rad CFX96 real-time PCR detection system using KAPA SYBR FAST qPCR kit (KAPA Biosystems). The relative expression levels of target genes were normalized to *ACTIN2* (*At3g18780*) levels. All primers used in RT-qPCR were listed in Table S1.

ChIP-PCR analysis—Inflorescences of four-week-old *pMP::MP-GFP, pMP::MP-HA,* and *pARF3::ARF3-GFP* transgenic plants were harvested and frozen in liquid nitrogen. One gram of inflorescences was used in ChIP experiments. The inflorescences were grinded to fine powder and then fixed with 1% formaldehyde (10 mM phosphate buffer, 0.1 M NaCl, 10 mM mercapto-ethanol, 1M hexylene glycol) for 10 min. Then 0.125 M glycine was added to stop the crosslink through incubate for 5 min. The solution was filtered through 4 layers of miracloth. Nuclei were isolated through centrifugation at 12,000 rpm for 10 min. The nuclei precipitate was rinsed for 3 times with buffer containing 10 mM phosphate buffer, 0.1 M NaCl, 10 mM mercapto-ethanol, 1 M hexylene glycol, 10 mM $MgCl_2$ and 0.5% Triton X-100. Nuclei were lysed with nuclei lysis buffer (50 mM Tris-HCl, pH8.0, 10 mM EDTA, 1% SDS). Protease inhititors were added in all the above liquids. The chromatin was sheared to an average size of 500 bp by sonication. The supernatant after centrifugation was used as input. Immunoprecipitations were performed using anti-GFP or anti-HA antibodies. No-antibody controls were used to calculate enrichment. PCR was performed using the precipitated DNA as templates. The enrichment of DNA fragments was determined by quantitative PCR analysis. Three independent biological repeats were performed for each ChIP analysis. All primers used in ChIP-PCR were listed in Table S1.

Yeast one-hybrid assay—To make the yeast one-hybrid assay bait constructs, promoter fragments of *WOX1* and *PRS* were amplified from genomic DNA using specific primers (see Supplementary Table 3). The PCR products were ligated into pAbAi vector (Clontech). Then the bait plasmids were linearized by *Bst*BI and integrated into yeast strain Y1HGOLD using PEG-mediated transformation according to the manufacturer's instructions (Yeast Hand Book; Clontech, PT3024-1). Transformants were selected on media lacking uracil, verified by PCR using a promoter-specific primer and a yeast chromosome primer, and

tested for auto-activation according to the manufacturer's instructions. All AD-TF prey clones were derived from pDEST22 (Life Technologies).

Yeast one-hybrid assay was performed according to the user manual of Matchmaker™ Gold Yeast One-Hybrid Library Screenig System (Clontech, 630491). Briefly, AD-TF plasmids were directly transformed into Y1HGOLD bait strains harboring genomic promoter-reporters through PEG-mediated transformation, and transformants were selected on media lacking uracil and tryptophan but containing 800 ng/ml aureobasidin A (AbA). An equal amount of transformed yeast culture was plated on medium lacking uracil and tryptophan without addition of AbA to control for transformation efficiency. Positive interactions were identified based on growth ability after transformation, on AbA-containing medium for 3 days. All interactions were validated by retesting using the same procedure.

In situ hybridizations (ISH)—ISH was performed on 8 μm paraffin sections. Details of methods used for fixation of plants, embedding in paraffin, and in situ hybridization can be found at http://www.its.caltech.edu/~plantlab/protocols/insitu.html. Sections were cut with a Leica RM2255 ortary microtome. *WOX1* and *PRS* probes were generated through amplifying of nucleotides 235 to 1030 of *WOX1* and 192 to 828 of *PRS* coding sequences by PCR with the forward primers 5'-CCGACACCAGATCAGTTAAG-3', 5'-GAATGCGGTGCAGATACAACA -3' and reverse primers 5'-CATAGAAACAGTGAATGCCA-3', 5'- GGTACTGTCTTGTTTGGAGT-3', respectively. The fragments were subsequently cloned into the pEASY-Blunt vector.

Tissue preparation for confocal analysis—Shoot apices with leaves removed were collected and immediately placed in 2.5% paraformaldehyde (PFA; Sigma-Aldrich) at pH 7.0 at 4°C, vacuum infiltrated for 30 min, and then were stored overnight at 4°C. Fixed tissue samples were washed with 10% (w/v) sucrose and 1% PFA at pH 7.0 for 20 min, 20% sucrose and 1% PFA at pH 7.0 for 20 min, and 30% sucrose and 1% PFA at pH 7.0 for 30 min, successively. Samples were then embedded in 5 to 7% (w/v) low melting point agarose (Promega) liquid gel at 30°C and placed at 4°C for 15 min to solidify. Sections of 50 μm were made using a Leica VT1000S vibratome. For high-resolution images, samples were stained with 50 μg/mL propidium iodide (PI, Sigma-Aldrich).

Live imaging—To dissect vegetative SAMs, seedlings grown under short-day conditions for 15 days were transferred to the dissecting medium (3% agarose) and fixed into a hole using forceps. Leaf primordia older than P_4 were carefully removed using a fine needle tip under a stereomicroscope (Nikon, SMZ18). FM4-64 (Thermo Fisher, 10 μg/mL) was applied to the SAM for 10 min. The dissected meristem with P_2 or P_3 was transferred to the imaging medium (1/2 MS medium with 1% agarose on the top) before live imaging. All live imaging was performed using 60× water dipping lens.

Confocal microscopy, optical microscopy, and scanning electron microscopy —Confocal images were taken with a Nikon A1 confocal microscope. Excitation and detection windows setups for GFP, Venus, and tdTomato were as described [17]. For imaging GFP and autofluorescence together, both were excited with a 488 nm laser and the emission was splited with a 500-550 nm band-pass filter for GFP and a 660-700 nm filter for

autofluorescence. To detect the signal of GFP together with FM4-64 or PI, 488 nm for GFP and 561 nm for FM4-64 or PI lasers were used for excitation, 500-530 nm band-pass filter for GFP and 570-620 nm band-pass filter for FM4-64 or PI were used for detection. For the combination of GFP, Venus and FM4-64, GFP and FM4-64 were detected together as described above and Venus was imaged alone using a 514 nm laser excitation and a 524-550 nm band-pass filter emission. Then the two scan results stacked together automatically. To image tdTomato, a 561 nm laser was used for excitation and a 570-620 nm band-pass filter was used for detection. All images were scanned with 1024 × 1024 pixels. All optical photographs were taken with a Nikon SMZ1000 stereoscopic microscope or an Olympus BX60 microscope equipped with a Nikon DS-Ri1 camera head. Scanning electron microscopy was performed using the Hitachi S-3000N variable pressure scanning electron microscopy.

Transient expression assays—The transient expression assay was performed in *N. benthamiana* leaves essentially as previously described [57]. The *WOX1* promoter was isolated using the forward primer 5'-GCGGTACCATGCTTGAAAATATCTCTGT-3' and the reverse primer 5'-CACTCGAGCTCTGGTTGCGTGTCGCATC-3' and cloned into pGL3-basic vector (Promega) at the *Kpn*I (5'-end) and *Xho*I (3'-end) sites upstream of *LUC*. The *WOX1* promoter with the mutated MP binding sites (*pWOX1Δ*) was amplified using the forward primer 5'-TCTCATATTCTTTTTAAAATTTATATTAATCT-3' and the reverse primer 5'-GATTAATATAAATTTTAAAAAGAATATGAGATCCC-3' from pGL3-pWOX1-LUC plasmid. Then the fused *pWOX1::LUC* and *pWOX1Δ::LUC* genes were subcloned into the *Kpn*I and *Bam*HI sites of pCAMBIA1300 vector. To generate *MP* effector construct, the *MP* cDNA was PCR amplified with the forward primer 5'-CACCCGGGATGATGGCTTCATTGTCTTG-3' and reverse primer 5'-CGACTAGTTTATGAAACAGAAGTCTTAA-3', and then was subcloned into the *Sma*I and *Spe*I sites downstream of the *p35S* promoter of the HA-pBA vector. For the *35S::mARF3* construct, the mutated form of *ARF3* cDNA was obtained as previously described [58] and subcloned into the *Sma*I and *Sac*I sites downstream of the *p35S* promoter of the HA-pBA vector.

The above constructs were transformed into GV3101 and the obtained *Agrobacterium* strains were used to infiltrate *N. benthamiana* leaves. Infiltrated plants were incubated at 22°C for 72 h before CCD imaging. The LUC images were captured using a low-light cooled CCD imaging apparatus (NightOWL II LB983 with indigo software). The transformed leaves were sprayed with 100 mM luciferin and placed in darkness for 5 min before luminescence detection. Error bars represent SD. Experiments were repeated at least five times.

Quantification and Statistical Analysis

For phenotypic quantification (as shown in Figure 2B, 3G, and 4K), leaf length and width were measured using the Nikon NIS-Elements software and the data were shown in mean ± SEM, and n indicates the number of leaves used for quantification. The details are as follows: Figure 2B: Col-0 cotyledon (n=12), *arf5-1* cotyledon (n=12), Col-0 rosette leaf (n=10), *arf5-1* rosette leaf (n=20). Figure 3G: WT (n=6), *wox1-2 prs* (n=6), *MPΔ* (n=6),

MPΔ wox1-2 (n=3), *MPΔ prs* (n=4). Figure 4K: Col-0 (n=24), *wox1-2 prs* (n=18), *pWOX1::WOX1* (n=24), *pWOX1Δ::WOX1* (n=18). Statistical analysis was performed through Student's *t* test in Excel and *P* values less than 0.05 was considered significant for any set of data.

Supplementary Material

Refer to Web version on PubMed Central for supplementary material.

ACKNOWLEDGMENTS

We thank Zhizhong Gong, Chun-Ming Liu, Michiel Vandenbussche, Dolf Weijers, and the ABRC for seeds. We thank Jiyan Qi and Ying Wang for assistance with imaging, and Ying Wang for comments on the manuscript. This research was supported by National Natural Science Foundation of China (NSFC) grant 31430010, National Basic Research Program of China grant 2014CB943500, and National Program for Support of Top-Notch Young Professionals to Y.J., NSFC grant 31401232 to C.G., National Institute of General Medical Sciences of the National Institutes of Health award R15GM114733 to N.T.K., and the State Key Laboratory of Plant Genomics.

REFERENCES

1. Waites R, and Hudson A. (1995). *phantastica*: a gene required for dorsoventrality of leaves in *Antirrhinum majus*. Development 121, 2143–2154.
2. Barton MK (2010). Twenty years on: the inner workings of the shoot apical meristem, a developmental dynamo. Dev Biol 341, 95–113. [PubMed: 19961843]
3. Bowman JL, and Floyd SK (2008). Patterning and polarity in seed plant shoots. Annu Rev Plant Biol 59, 67–88. [PubMed: 18031217]
4. Braybrook SA, and Kuhlemeier C. (2010). How a plant builds leaves. Plant Cell 22, 1006–1018. [PubMed: 20424178]
5. Efroni I, Eshed Y, and Lifschitz E. (2010). Morphogenesis of simple and compound leaves: a critical review. Plant Cell 22, 1019–1032. [PubMed: 20435903]
6. Husbands AY, Chitwood DH, Plavskin Y, and Timmermans MC (2009). Signals and prepatterns: new insights into organ polarity in plants. Genes Dev 23, 1986–1997. [PubMed: 19723761]
7. Xu L, Yang L, and Huang H. (2007). Transcriptional, post-transcriptional and post-translational regulations of gene expression during leaf polarity formation. Cell Res 17, 512–519. [PubMed: 17549070]
8. Chitwood DH, Nogueira FT, Howell MD, Montgomery TA, Carrington JC, and Timmermans MC (2009). Pattern formation via small RNA mobility. Genes Dev 23, 549–554. [PubMed: 19270155]
9. Fahlgren N, Montgomery TA, Howell MD, Allen E, Dvorak SK, Alexander AL, and Carrington JC (2006). Regulation of *AUXIN RESPONSE FACTOR3* by TAS3 ta-siRNA affects developmental timing and patterning in *Arabidopsis*. Curr Biol 16, 939–944. [PubMed: 16682356]
10. Garcia D, Collier SA, Byrne ME, and Martienssen RA (2006). Specification of leaf polarity in *Arabidopsis* via the *trans*-acting siRNA pathway. Curr Biol 16, 933–938. [PubMed: 16682355]
11. Pekker I, Alvarez JP, and Eshed Y. (2005). Auxin response factors mediate *Arabidopsis* organ asymmetry via modulation of KANADI activity. Plant Cell 17, 2899–2910. [PubMed: 16199616]
12. Nogueira FT, Madi S, Chitwood DH, Juarez MT, and Timmermans MC (2007). Two small regulatory RNAs establish opposing fates of a developmental axis. Genes Dev 21, 750–755. [PubMed: 17403777]
13. Yao X, Wang H, Li H, Yuan Z, Li F, Yang L, and Huang H. (2009). Two types of *cis*-acting elements control the abaxial epidermis-specific transcription of the *MIR165a* and *MIR166a* genes. FEBS Lett 583, 3711–3717. [PubMed: 19879265]
14. Tatematsu K, Toyokura K, Miyashima S, Nakajima K, and Okada K. (2015). A molecular mechanism that confines the activity pattern of miR165 in *Arabidopsis* leaf primordia. Plant J 82, 596–608. [PubMed: 25788175]

15. Juarez MT, Kui JS, Thomas J, Heller BA, and Timmermans MC (2004). microRNA-mediated repression of *rolled leaf1* specifies maize leaf polarity. Nature 428, 84–88. [PubMed: 14999285]
16. Mallory AC, Reinhart BJ, Jones-Rhoades MW, Tang G, Zamore PD, Barton MK, and Bartel DP (2004). MicroRNA control of *PHABULOSA* in leaf development: importance of pairing to the microRNA 5' region. EMBO J 23, 3356–3364. [PubMed: 15282547]
17. Qi J, Wang Y, Yu T, Cunha A, Wu B, Vernoux T, Meyerowitz E, and Jiao Y. (2014). Auxin depletion from leaf primordia contributes to organ patterning. Proc Natl Acad Sci U S A 111, 18769–18774. [PubMed: 25512543]
18. Hagemann W, and Gieissberg S. (1996). Organogenetic capacity of leaves: The significance of marginal blastozones in angiosperms. Plant Syst Evol 199, 121–152.
19. Nardmann J, and Werr W. (2013). Symplesiomorphies in the WUSCHEL clade suggest that the last common ancestor of seed plants contained at least four independent stem cell niches. New Phytol 199, 1081–1092. [PubMed: 23721178]
20. Ichihashi Y, and Tsukaya H. (2015). Behavior of leaf meristems and their modification. Front Plant Sci 6, 1060. [PubMed: 26648955]
21. Alvarez JP, Furumizu C, Efroni I, Eshed Y, and Bowman JL (2016). Active suppression of a leaf meristem orchestrates determinate leaf growth. eLife 5, e15023. [PubMed: 27710768]
22. Nakata M, Matsumoto N, Tsugeki R, Rikirsch E, Laux T, and Okada K (2012). Roles of the middle domain-specific *WUSCHEL-RELATED HOMEOBOX* genes in early development of leaves in *Arabidopsis*. Plant Cell 24, 519–535. [PubMed: 22374393]
23. Vandenbussche M, Horstman A, Zethof J, Koes R, Rijpkema AS, and Gerats T (2009). Differential recruitment of WOX transcription factors for lateral development and organ fusion in Petunia and *Arabidopsis*. Plant Cell 21, 2269–2283. [PubMed: 19717616]
24. Tadege M, Lin H, Bedair M, Berbel A, Wen J, Rojas CM, Niu L, Tang Y, Sumner L, Ratet P, et al. (2011). *STENOFOLIA* regulates blade outgrowth and leaf vascular patterning in *Medicago truncatula* and *Nicotiana sylvestris*. Plant Cell 23, 2125–2142. [PubMed: 21719692]
25. Nardmann J, Ji J, Werr W, and Scanlon MJ (2004). The maize duplicate genes *narrow sheath1* and *narrow sheath2* encode a conserved homeobox gene function in a lateral domain of shoot apical meristems. Development 131, 2827–2839. [PubMed: 15169755]
26. Laux T, Mayer KF, Berger J, and Jurgens G (1996). The *WUSCHEL* gene is required for shoot and floral meristem integrity in *Arabidopsis*. Development 122, 87–96. [PubMed: 8565856]
27. Lin H, Niu L, McHale NA, Ohme-Takagi M, Mysore KS, and Tadege M (2013). Evolutionarily conserved repressive activity of WOX proteins mediates leaf blade outgrowth and floral organ development in plants. Proc Natl Acad Sci U S A 110, 366–371. [PubMed: 23248305]
28. Shimizu R, Ji J, Kelsey E, Ohtsu K, Schnable PS, and Scanlon MJ (2009). Tissue specificity and evolution of meristematic WOX3 function. Plant Physiol 149, 841–850. [PubMed: 19073779]
29. Dolzblasz A, Nardmann J, Clerici E, Causier B, van der Graaff E, Chen J, Davies B, Werr W, and Laux T (2016). Stem cell regulation by *Arabidopsis WOX* genes. Mol Plant 9, 1028–1039. [PubMed: 27109605]
30. Krogan NT, and Berleth T (2012). A dominant mutation reveals asymmetry in MP/ARF5 function along the adaxial-abaxial axis of shoot lateral organs. Plant Signal Behav 7, 940–943. [PubMed: 22751359]
31. Donnelly PM, Bonetta D, Tsukaya H, Dengler RE, and Dengler NG (1999). Cell cycling and cell enlargement in developing leaves of *Arabidopsis*. Dev Biol 215, 407–419. [PubMed: 10545247]
32. Guilfoyle TJ, and Hagen G (2007). Auxin response factors. Curr Opin Plant Biol 10, 453–460. [PubMed: 17900969]
33. Wang Y, Wang J, Shi B, Yu T, Qi J, Meyerowitz EM, and Jiao Y (2014). The stem cell niche in leaf axils is established by auxin and cytokinin in *Arabidopsis*. Plant Cell 26, 2055–2067. [PubMed: 24850849]
34. Liao CY, Smet W, Brunoud G, Yoshida S, Vernoux T, and Weijers D. (2015). Reporters for sensitive and quantitative measurement of auxin response. Nat Methods 12, 207–210. [PubMed: 25643149]

35. Sarojam R, Sappl PG, Goldshmidt A, Efroni I, Floyd SK, Eshed Y, and Bowman JL (2010). Differentiating *Arabidopsis* shoots from leaves by combined YABBY activities. Plant Cell 22, 2113–2130. [PubMed: 20628155]
36. Ohta M, Matsui K, Hiratsu K, Shinshi H, and Ohme-Takagi M. (2001). Repression domains of class II ERF transcriptional repressors share an essential motif for active repression. Plant Cell 13, 1959–1968. [PubMed: 11487705]
37. Konishi M, Donner TJ, Scarpella E, and Yanagisawa S (2015). MONOPTEROS directly activates the auxin-inducible promoter of the Dof5.8 transcription factor gene in Arabidopsis thaliana leaf provascular cells. J. Exp. Bot 66, 283–291. [PubMed: 25336688]
38. Boer DR, Freire-Rios A, van den Berg WA, Saaki T, Manfield IW, Kepinski S, Lopez-Vidrieo I, Franco-Zorrilla JM, de Vries SC, Solano R, et al. (2014). Structural basis for DNA binding specificity by the auxin-dependent ARF transcription factors. Cell 156, 577–589. [PubMed: 24485461]
39. Schlereth A, Moller B, Liu W, Kientz M, Flipse J, Rademacher EH, Schmid M, Jurgens G, and Weijers D. (2010). MONOPTEROS controls embryonic root initiation by regulating a mobile transcription factor. Nature 464, 913–916. [PubMed: 20220754]
40. Allen E, Xie Z, Gustafson AM, and Carrington JC (2005). MicroRNA-directed phasing during trans-acting siRNA biogenesis in plants. Cell 121, 207–221. [PubMed: 15851028]
41. Williams L, Carles CC, Osmont KS, and Fletcher JC (2005). A database analysis method identifies an endogenous trans-acting short-interfering RNA that targets the *Arabidopsis ARF2, ARF3,* and *ARF4* genes. Proc Natl Acad Sci U S A 102, 9703–9708. [PubMed: 15980147]
42. Okushima Y, Mitina I, Quach HL, and Theologis A (2005). AUXIN RESPONSE FACTOR 2 (ARF2): a pleiotropic developmental regulator. Plant J. 43, 29–46. [PubMed: 15960614]
43. Okushima Y, Overvoorde PJ, Arima K, Alonso JM, Chan A, Chang C, Ecker JR, Hughes B, Lui A, Nguyen D, et al. (2005). Functional genomic analysis of the *AUXIN RESPONSE FACTOR* gene family members in *Arabidopsis thaliana*: unique and overlapping functions of *ARF7* and *ARF19*. Plant Cell 17, 444–463. [PubMed: 15659631]
44. Ulmasov T, Liu ZB, Hagen G, and Guilfoyle TJ (1995). Composite structure of auxin response elements. Plant Cell 7, 1611–1623. [PubMed: 7580254]
45. Alvarez JP, Pekker I, Goldshmidt A, Blum E, Amsellem Z, and Eshed Y (2006). Endogenous and synthetic microRNAs stimulate simultaneous, efficient, and localized regulation of multiple targets in diverse species. Plant Cell 18, 1134–1151. [PubMed: 16603651]
46. Liu X, Dinh TT, Li D, Shi B, Li Y, Cao X, Guo L, Pan Y, Jiao Y, and Chen X. (2014). AUXIN RESPONSE FACTOR 3 integrates the functions of AGAMOUS and APETALA2 in floral meristem determinacy. Plant J. 80, 629–641. [PubMed: 25187180]
47. McHale NA, and Marcotrigiano M (1998). *LAM1* is required for dorsoventrality and lateral growth of the leaf blade in *Nicotiana*. Development 125, 4235–4243. [PubMed: 9753678]
48. Müller CJ, Valdés AE, Wang G, Ramachandran P, Beste L, Uddenberg D, and Carlsbecker A. (2016). PHABULOSA mediates an auxin signaling loop to regulate vascular patterning in *Arabidopsis*. Plant Physiol 170, 956–970. [PubMed: 26637548]
49. Bhatia N, Bozorg B, Larsson A, Ohno C, Jönsson H, and Heisler MG (2016). Auxin acts through MONOPTEROS to regulate plant cell polarity and pattern phyllotaxis. Curr Biol 26, 3202–3208. [PubMed: 27818174]
50. Krogan NT, Marcos D, Weiner AI, and Berleth T. (2016). The auxin response factor MONOPTEROS controls meristem function and organogenesis in both the shoot and root through the direct regulation of PIN genes. New Phytol 212, 42–50. [PubMed: 27441727]
51. Rademacher EH, Moller B, Lokerse AS, Llavata-Peris CI, van den Berg W, and Weijers D. (2011). A cellular expression map of the Arabidopsis AUXIN RESPONSE FACTOR gene family. Plant J. 68, 597–606. [PubMed: 21831209]
52. Vernoux T, Brunoud G, Farcot E, Morin V, Van den Daele H, Legrand J, Oliva M, Das P, Larrieu A, Wells D, et al. (2011). The auxin signalling network translates dynamic input into robust patterning at the shoot apex. Mol Syst Biol 7, 508. [PubMed: 21734647]

53. Benkova E, Michniewicz M, Sauer M, Teichmann T, Seifertova D, Jurgens G, and Friml J. (2003). Local, efflux-dependent auxin gradients as a common module for plant organ formation. Cell 115, 591–602. [PubMed: 14651850]

54. Xu TT, Ren SC, Song XF, and Liu CM (2015). CLE19 expressed in the embryo regulates both cotyledon establishment and endosperm development in *Arabidopsis*. J Exp Bot 66, 5217–5227. [PubMed: 26071532]

55. Wang L, Hua D, He J, Duan Y, Chen Z, Hong X, and Gong Z. (2011). Auxin Response Factor2 (ARF2) and its regulated homeodomain gene HB33 mediate abscisic acid response in Arabidopsis. PLoS Genet. 7, e1002172. [PubMed: 21779177]

56. Clough SJ, and Bent AF (1998). Floral dip: a simplified method for *Agrobacterium*-mediated transformation of *Arabidopsis thaliana*. Plant J 16, 735–743. [PubMed: 10069079]

57. Sun J, Qi L, Li Y, Chu J, and Li C. (2012). PIF4-mediated activation of *YUCCA8* expression integrates temperature into the auxin pathway in regulating *Arabidopsis* hypocotyl growth. PLoS Genet 8, e1002594. [PubMed: 22479194]

58. Yifhar T, Pekker I, Peled D, Friedlander G, Pistunov A, Sabban M, Wachsman G, Alvarez JP, Amsellem Z, and Eshed Y. (2012). Failure of the tomato *trans*-acting short interfering RNA program to regulate *AUXIN RESPONSE FACTOR3* and *ARF4* underlies the wiry leaf syndrome. Plant Cell 24, 3575–3589. [PubMed: 23001036]

Highlights

- Adaxial-expressed *MP* and abaxial-enriched auxin define middle domain *WOX* expression.
- Redundant abaxial-enriched ARF repressors suppress *WOX* expression.
- Spatial auxin signaling transforms adaxial-abaxial polarity into leaf flattening.

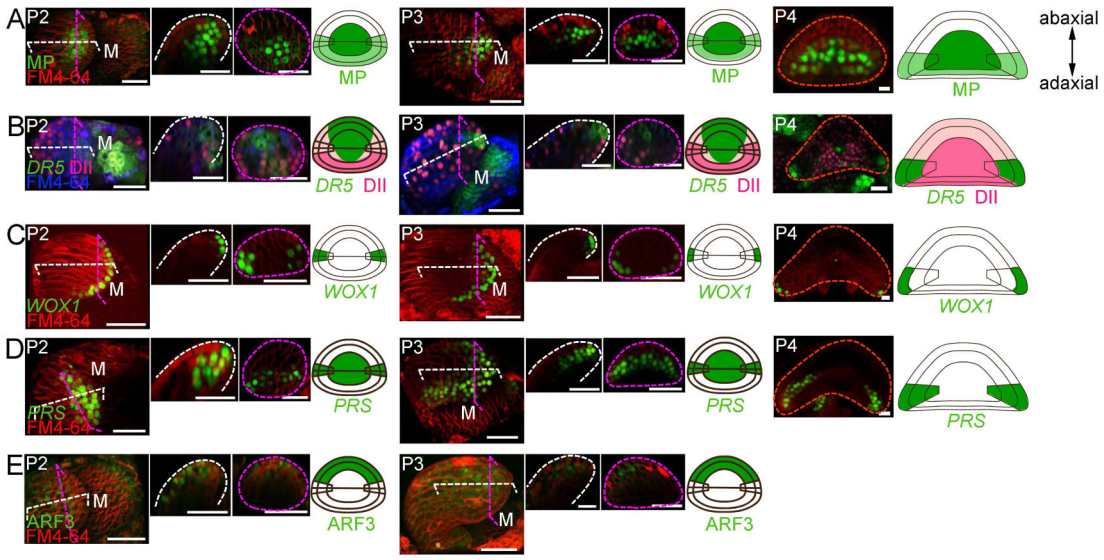

Figure 1. Spatially defined auxin signaling in the marginal and middle domains.

Optical and agarose sections through P_2, P_3, and P_4 of vegetative shoot apices showing expression of (**A**) MP-GFP (green), (**B**) *pDR5::GFPer* (green) and DII-Venus (magenta), (**C**) *pWOX1::GFP* (green), (**D**) *pPRS::GFP* (green), and (**E**) ARF3-GFP (green). The left and middle panels, maximum intensity projections and optical sections of live imaging results with FM4-64 staining. White dotted lines indicate longitudinal sections. Pink dotted lines indicate transverse sections. The right panels, agarose sections with PI staining. Note the *pWOX1::GFP* reporter may have narrower expression domain than results obtained by ISH (Figures 3C and 5B). Scale bars, 20 μm. See also Figure S1.

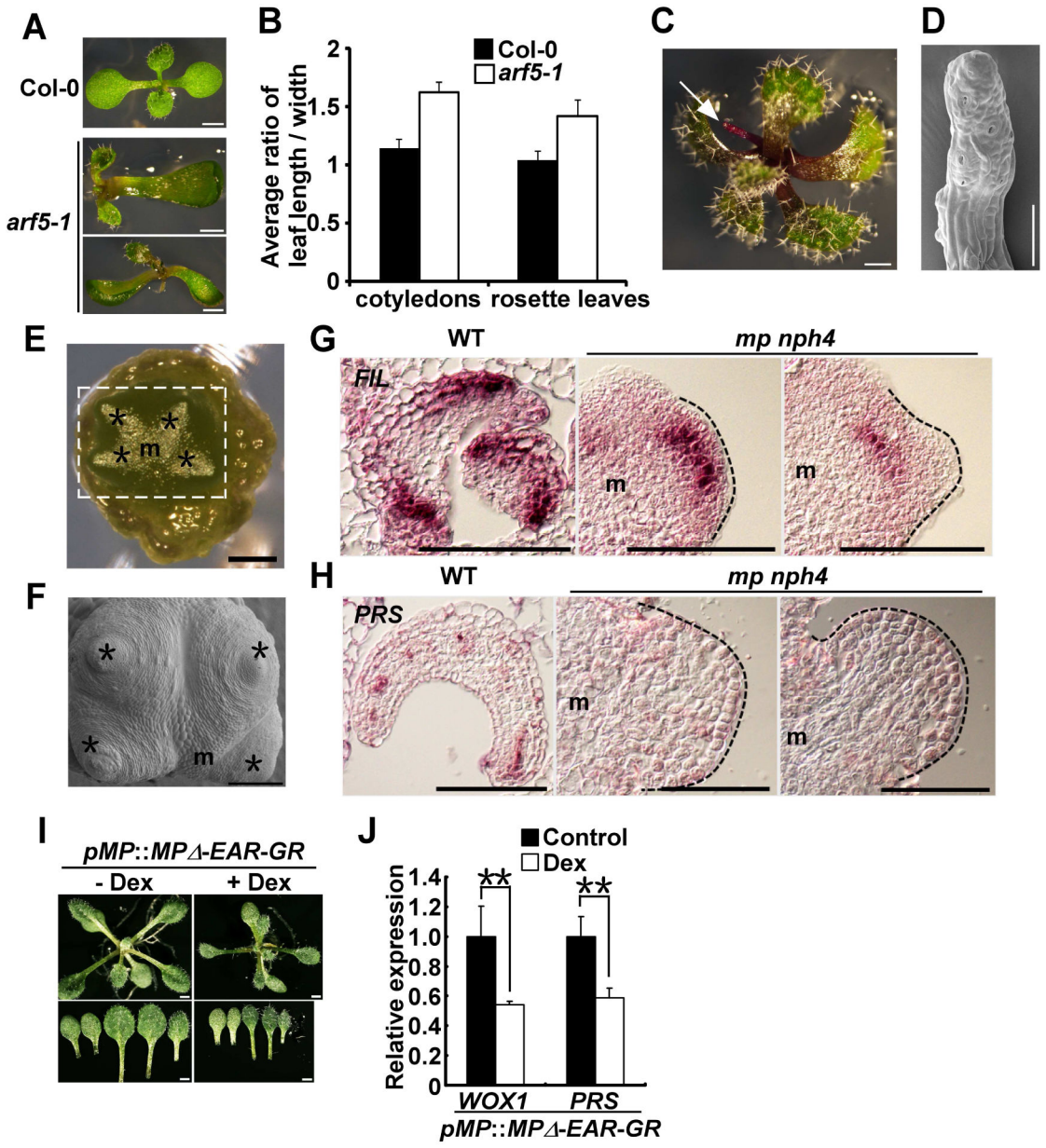

Figure 2. *MP* regulates leaf patterning and expression of *WOX* genes.

(A) Five-day-old *arf5-1* seedlings. Top, wild-type. Middle, *arf5-1* with one cotyledon. Bottom, *arf5-1* with two cotyledons. Scale bars, 1 mm.

(B) Quantification of length-width ratio of *arf5-1* cotyledons and rosette leaves. Data are presented as mean ± SD for more than three independent experiments.

(C) A seventeen-day-old *arf5-1* seedling. White arrow indicates a needle-like rosette leaf. Scale bar, 1 mm.

(D) Scanning electron micrograph (SEM) analysis of the needle-like rosette leaf indicated by white arrow in (C). Scale bar, 100 μm.

(E) A seventeen-day-old *mp nph4* seedling. Dark stars indicate leaf primordium-like bulges. Scale bar, 300 μm.

(F) SEM analysis of the shoot apical meristem indicated by white dotted box in (E). Scale bar, 300 μm.
(G) *FIL* transcript accumulation in transverse sections of *mp nph4* leaf primordium-like bulge (dark dotted lines). Scale bars, 50 μm.
(H) *PRS* transcript accumulation in transverse sections of *mp nph4* leaf primordium-like bulge (dark dotted lines). Scale bars, 50 μm.
(I) Vegetative and rosette leaf phenotypes of two-week-old *pMP::MPΔ-EAR-GR* transgenic plants without or with Dex treatment. Scale bars, 1 mm.
(J) RT-qPCR analysis of *WOX1* and *PRS* expression in *pMP::MPΔ-EAR-GR* vegetative meristems. Data are presented as mean ± SD for more than three independent experiments. $^{**}P < 0.01$. m, meristem. r, rosette leaf, c, cotyledon. See also Figure S2.

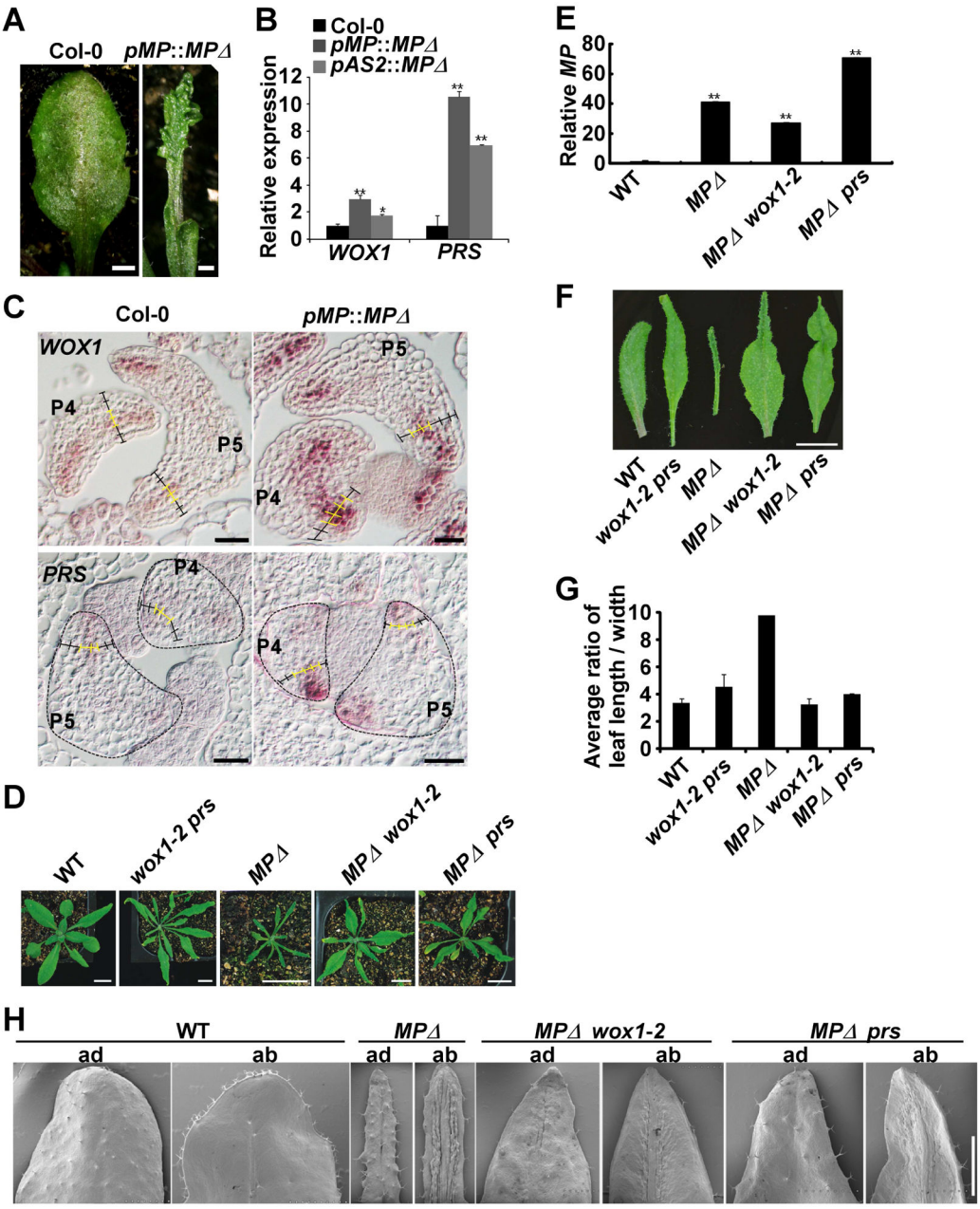

Figure 3. *MP* activates *WOX1* and *PRS* expression in the marginal and middle domains.

(A) Rosette leaf phenotypes of Col-0 and *pMP::MPΔ* plants. Scale bars, 1 mm.

(B) RT-qPCR analysis of *WOX1* and *PRS* expression in *pMP::MPΔ* and *pAS2::MPΔ* transgenic rosette leaves. Data are presented as mean ± SD for more than three independent experiments. $*P < 0.05$; $**P < 0.01$.

(C) Comparison of the *WOX1* and *PRS* transcript accumulation in transverse sections of P_4 and P_5 leaf primordia of wild-type and *pMP::MPΔ* transgenic plants through ISH. Ladders colored in yellow indicate *WOX1* and *PRS* expressing cells. Note expansion of expression domains and enhancement of expression levels in *pMP::MPΔ* plants. Scale bars, 20 μm.

(D) Vegetative phenotypes of one-month-old wild-type, *wox1-2 prs, pMP::MPΔ, pMP::MPΔ wox1-2*, and *pMP::MPΔ prs* plants. Scale bars, 10 mm.
(E) Relative expression levels of *MP* in plants shown in (D). Data are presented as mean ± SD for two independent transgenic progenies. $^{**}P < 0.01$.
(F) The fourth rosette leaves of plants shown in (D). Scale bar, 10 mm.
(G) Quantification of length-width ratio of leaves shown in (F).
(H) SEM analysis of the fourth rosette leaves of wild-type, *pMP::MPΔ, pMP::MPΔ wox1-2,* and *pMP::MPΔ prs* plants. ad, adaxial; ab, abaxial. Scale bar, 2 mm.
See also Figure S3.

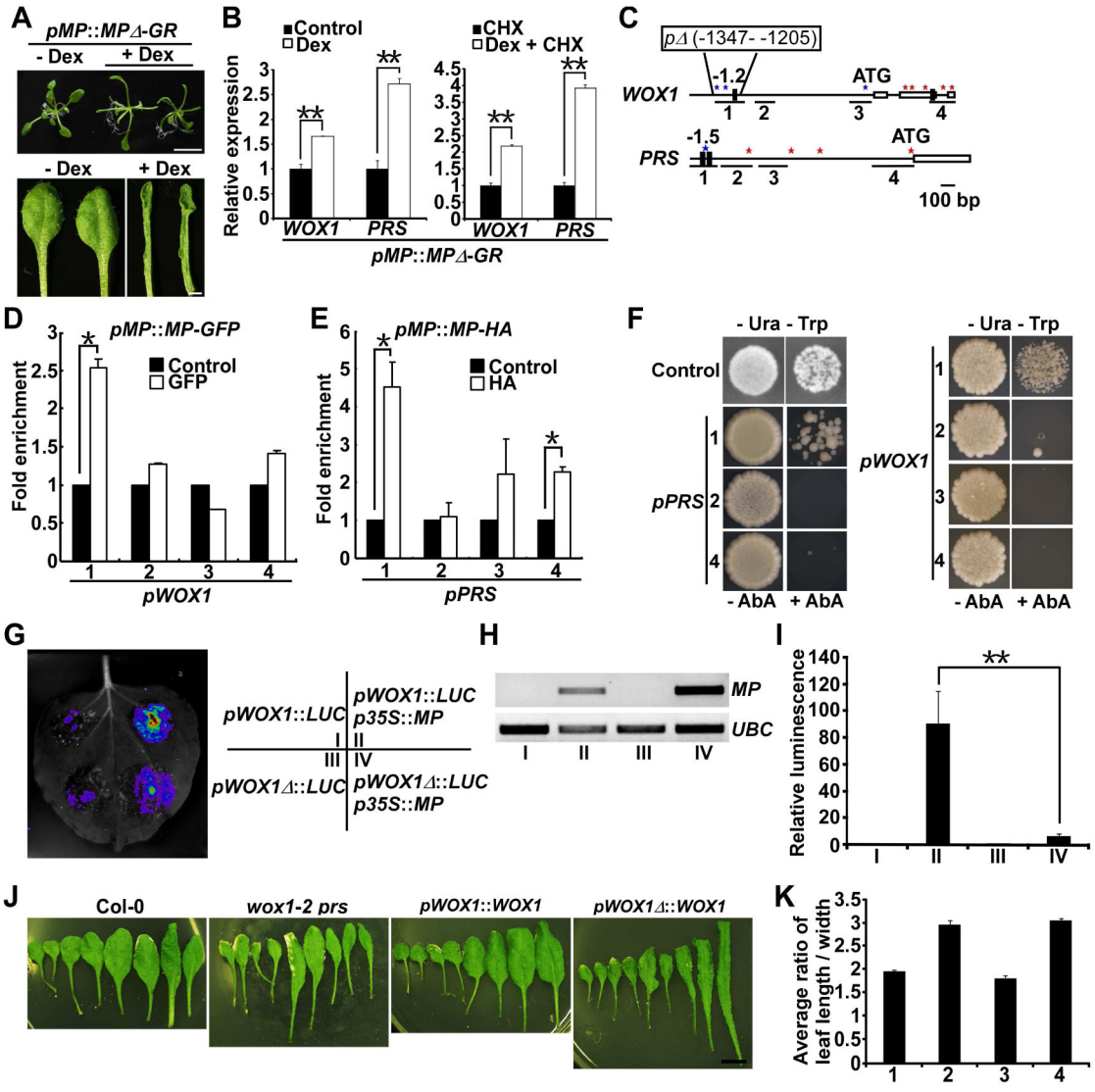

Figure 4. MP directly binds to the *WOX1* and *PRS* genomic regions.

(A) Vegetative and rosette leaf phenotypes of two-week-old *pMP::MPΔ-GR* transgenic plants. Scale bars, 10 mm (top) or 1 mm (bottom).

(B) RT-qPCR analysis of *WOX1* and *PRS* expression in *pMP::MPΔ-GR* shoot apices. Data are presented as mean ± SD for more than three independent experiments. $^{**}P < 0.01$.

(C) Schematic of the *WOX1* and *PRS* genomic regions. Black boxes indicate AuxRE pairs (Boer et al., 2014), and stars indicate single AuxRE sites. Red stars represent TGTCGN or TGTCTG, and blue stars represent TGTCTC. The underlying lines represent the DNA fragments amplified in ChIP assays, or used for Y1H analysis. *pΔ* (-1347 - -1205) in white box indicates the promoter region deleted in *pWOX1Δ::WOX1* construct in (J).

(D) Anti-GFP ChIP enrichment of *WOX1* genomic fragments using *pMP::MP-GFP* inflorescences.

(E) Anti-HA ChIP enrichment of *PRS* genomic fragments using *pMP::MP-HA* inflorescences.

(F) Y1H assay of MP with *WOX1* and *PRS* genomic fragments indicated in (C). Note fragment 3 of *PRS* was excluded due to strong self-activation in yeast.
(G) Transient expression assay showing MP activation of *WOX1* expression. A representative image of *N. benthamiana* leaves 72 h after infiltration is shown. The right panel indicates the infiltrated constructs.
(H) RT-PCR analysis of *MP* expression in the infiltrated leaf areas shown in (G). Total RNA was extracted from leaf areas of *N. benthamiana* coinfiltrated with different constructs.
(I) Quantitative analysis of luminescence intensity in (G). Five independent replicates were performed. Data are presented as mean ± SD for more than three independent experiments. $*P < 0.05$.
(J) Rosette leaves of thirty-day-old Col-0, *wox1-2 prs, pWOX1::WOX1,* and *pWOX1Δ::WOX1* transgenic plants in *wox1-2 prs* backgrounds. Scale bar, 10 mm.
(K) Quantification of length-width ratio of all rosette leaves of thirty-day-old plants. 1, 2, 3 and 4 indicate Col-0, *wox1-2 prs, pWOX1::WOX1 wox1-2 prs,* and *pWOX1Δ::WOX1 wox1-2 prs* transgenic plants, respectively.
See also Figure S4.

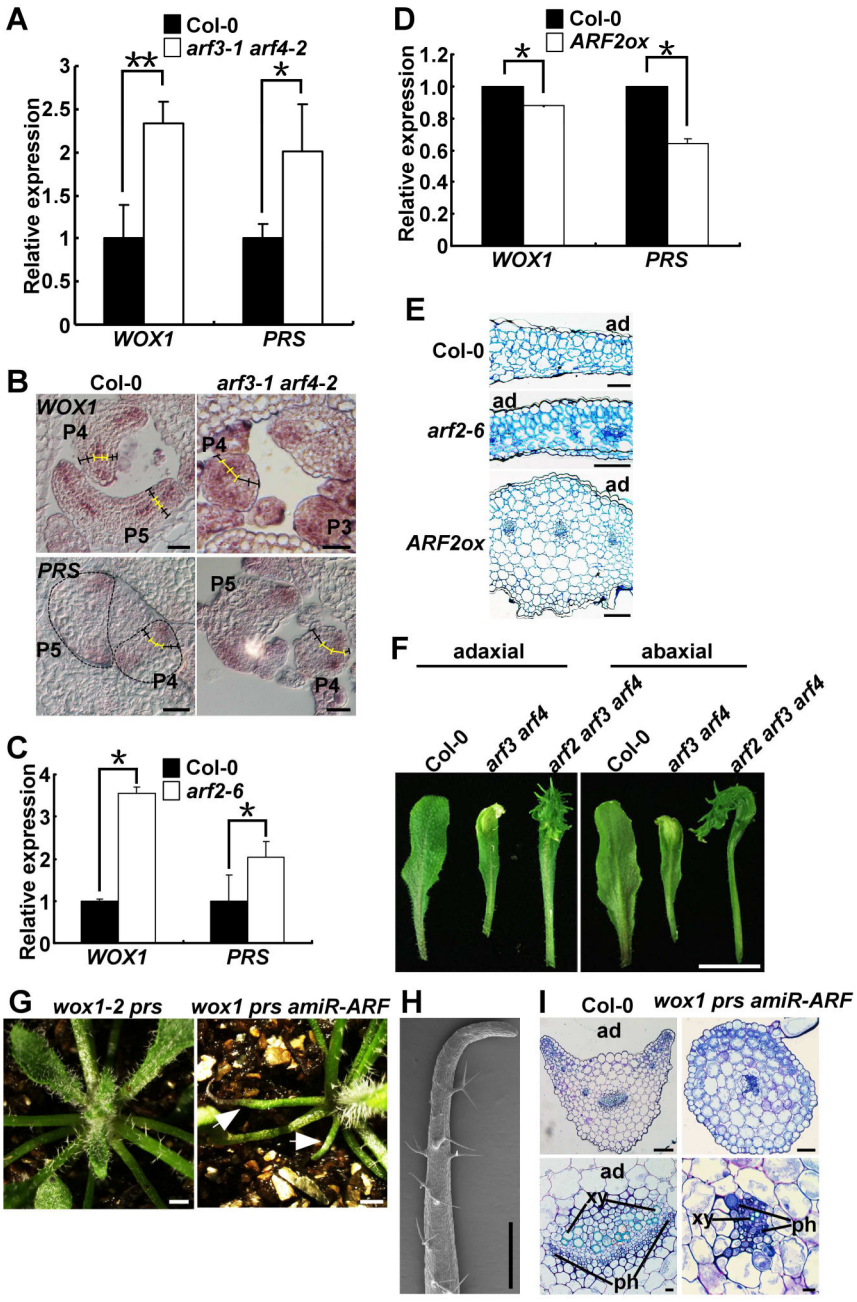

Figure 5. TAS3-targeted ARFs inhibit *WOX1* and *PRS* expression in the abaxial domain.

(A) RT-qPCR analysis of *WOX1* and *PRS* expression in Col-0 and *arf3-1 arf4-2* rosette leaves. Data are presented as mean ± SD for more than three independent experiments. *$P <$ 0.05, **$P < 0.01$.

(B) Comparison of the *WOX1* and *PRS* transcript accumulation in transverse sections of P_4 and P_5 leaf primordia of Col-0 and *arf3-1 arf4-2* mutants through ISH. Ladders colored in yellow indicate *WOX1* and *PRS* expressed cells. Note expansion of expression domains and enhancement of expression levels in *pMP::MPΔ* plants. Scale bar, 20 μm.

(C) RT-qPCR analysis of *WOX1* and *PRS* expression in Col-0 and *arf2-6* rosette leaves. Data are presented as mean ± SD for more than three independent experiments. $*P < 0.05$.
(D) RT-qPCR analysis of *WOX1* and *PRS* expression in Col-0 and *ARF2ox* transgenic rosette leaves. Data are presented as mean ± SD for more than three independent experiments. $*P < 0.05$.
(E) Cross section analysis of wild-type, *arf2-6,* and *ARF2ox* rosette leaves. Ad, adaxial. Scale bar, 100 μm.
(F) Rosette leaf phenotypes of *arf3-1 arf4-2* double and *arf3-1 arf4-2 arf2-6* triple mutants. Scale bar, 10 mm.
(G) Phenotypes of *wox1-2 prs p35S::amiR-ARF* rosette leaves. White arrows indicate needle-like leaves in *wox1-2 prs p35S::amiR-ARF* plants. Scale bars, 10 mm.
(H) SEM analysis of the needle-like rosette leaf indicated by white arrow in (G). Scale bar, 500 μm.
(I) Cross section of Col-0 and *wox1-2 prs p35S::amiR-ARF* leaf petioles. Scale bars, 100 μm (top) or 10 μm (bottom). ad, adaxial; xy, xylem; ph, phloem.
See also Figure S5 and S6.

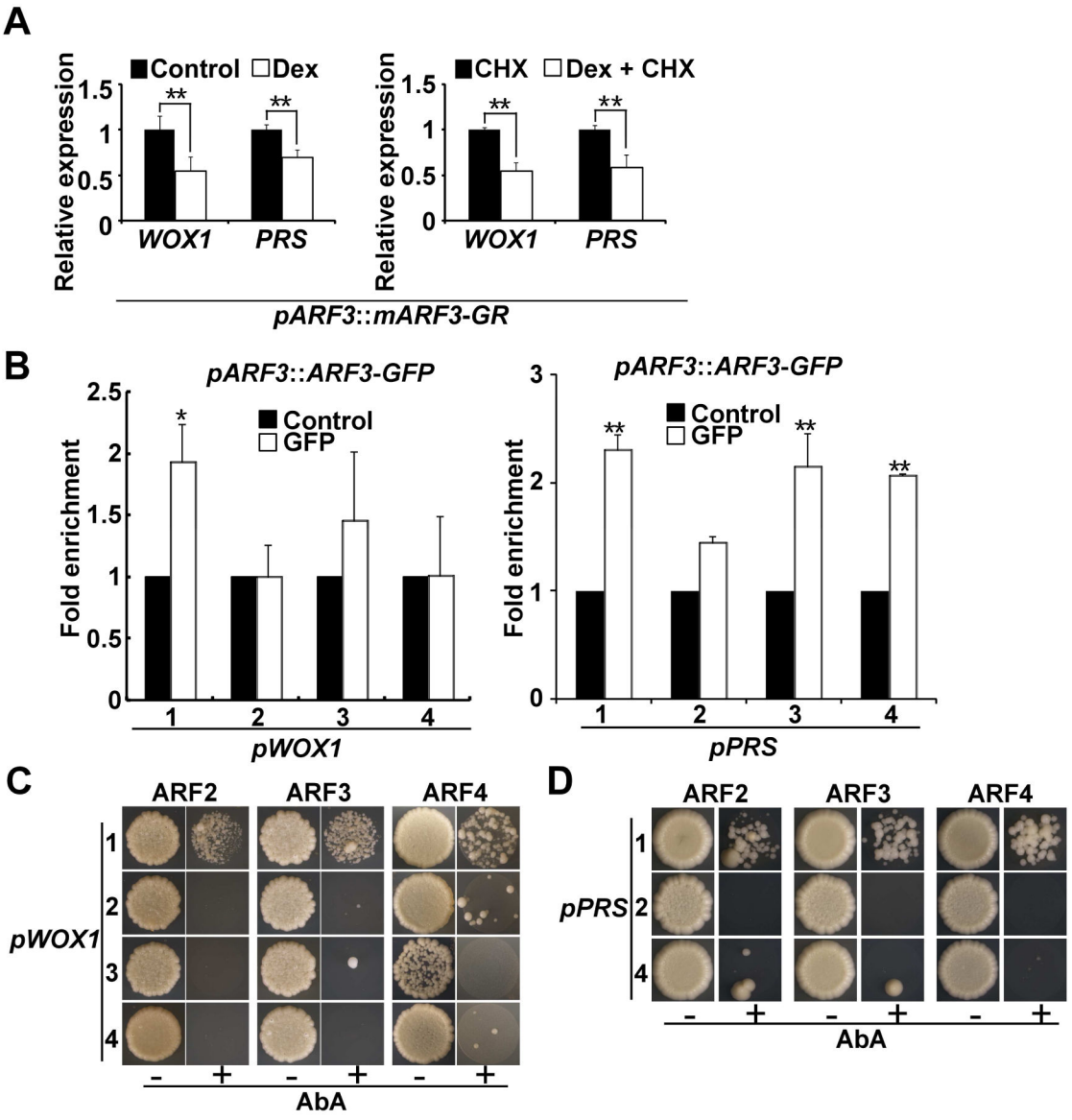

Figure 6. TAS3-targeted ARFs directly bind to the *WOX1* and *PRS* genomic regions.

(A) RT-qPCR analysis of *WOX1* and *PRS* expression in *pARF3::mARF3-GR* vegetative apices. Data are presented as mean ± SD for more than three independent experiments. $^{**}P < 0.01$.

(B) Anti-GFP ChIP enrichment of *WOX1* and *PRS* genomic fragments using *pARF3::ARF3-GFP* inflorescences. $^{*}P < 0.05$, $^{**}P < 0.01$.

(C and D) Y1H assay of ARF2, ARF3 and ARF4 with *WOX1* (B) and *PRS* (C) genomic fragments indicated in Figure 4C. Note fragment 3 of *PRS* was excluded due to strong self-activation in yeast.

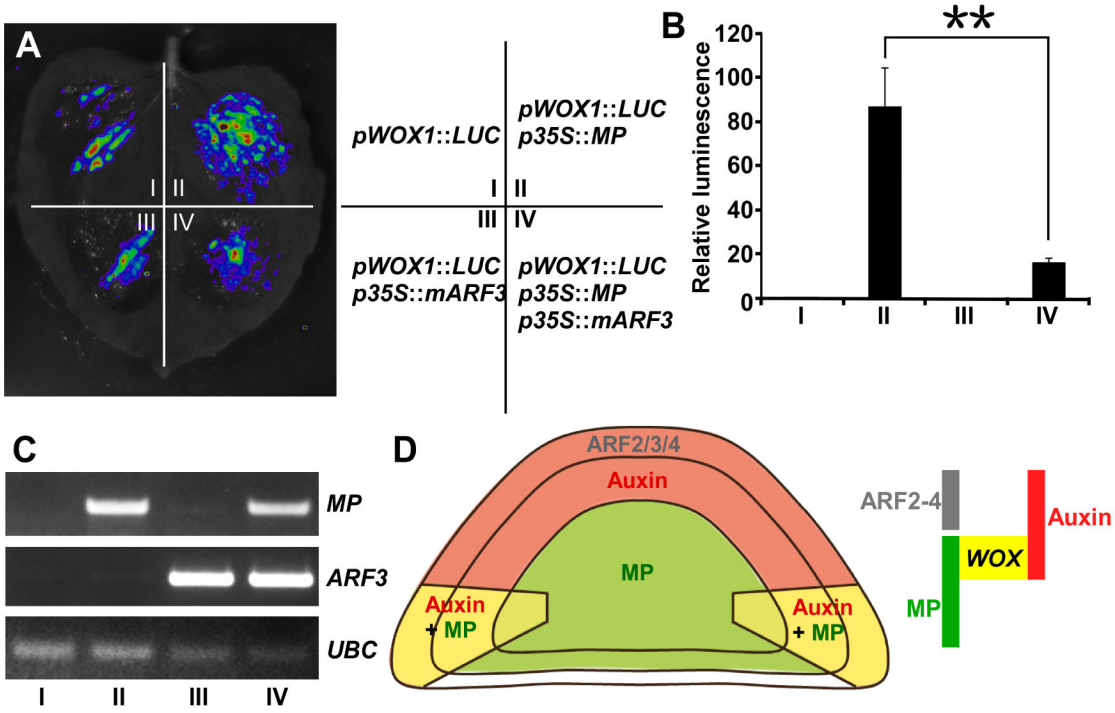

Figure 7. MP and ARF3 play antagonistic roles in regulating *WOX1* expression.

(A) Transient expression assay showing MP activates *WOX1* while ARF3 antagonizes MP effect on the expression of *WOX1.* Representative image of a *N. benthamiana* leaf 72 h after infiltration was shown. The right panel indicates the infiltrated constructs.

(B) Quantitative analysis of luminescence intensity in (A). Five independent replicates were performed. Data are presented as mean ± SD for more than three independent experiments. $^{**}P < 0.01$.

(C) RT-PCR analysis of *MP* and *ARF3* expression in the infiltrated leaf areas indicated in (A).

(D) Conceptual model of how spatial auxin signaling controls leaf patterning in leaf primordium.